

On Filtering Schemes in the Quantum-Classical Liouville Approach to Non-adiabatic Dynamics

Daniel Uken

*School of Chemistry and Physics, University of KwaZulu-Natal
Private Bag X01, Scottsville 3209 Pietermaritzburg, South Africa*

Alessandro Sergi

*School of Chemistry and Physics, University of KwaZulu-Natal
Private Bag X01, Scottsville 3209 Pietermaritzburg and National
Institute for Theoretical Physics (NITheP), KwaZulu-Natal, South Africa*

Francesco Petruccione

*School of Chemistry and Physics and National Institute for Theoretical Physics,
University of KwaZulu-Natal, Westville Campus,
Private Bag X54001, Durban 4000,
South Africa and National Institute for Theoretical
Physics (NITheP), KwaZulu-Natal, South Africa*

Abstract

We study a number of filtering schemes for the reduction of the statistical error in non-adiabatic calculations by means of the quantum-classical Liouville equation. In particular, we focus on a scheme based on setting a threshold value on the sampling weights, so that when the threshold is overcome the value of the weight is reset, and on another approach which prunes the ensemble of the allowed non-adiabatic transitions according to a generalised sampling probability. Both methods have advantages and drawbacks, however their combination drastically improves the performance of an algorithm known as the Sequential Short Time Step Propagation [D. MacKernan et al., J. Phys: Condens. Matter **14** 9069 (2002)], which is derived from a simple first order expansion of the quantum-classical propagator. Such an algorithm together with the combined filtering procedures produce results that compare very well with those obtained by means of numerically “exact” quantum calculations for the spin-boson model, even for intermediate and strong coupling regimes.

I. INTRODUCTION

In the field of condensed matter, many systems can be modeled using a quantum subsystem coupled to a classical bath. When energy is free to be exchanged between the subsystem and the bath, the resulting dynamics is known to be non-adiabatic. This type of dynamics is very difficult to simulate due to the quantum back-reaction of the subsystem onto the bath [1–5]. A number of numerical methods have been proposed for the calculation of non-adiabatic dynamics on a computer, the most common of which are so-called surface hopping schemes [6–12]. More recently, an approach based on the quantum-classical Liouville equation has been applied with success to condensed matter systems [13–19]. This approach allows one to construct a proper formulation of the statistical mechanics of quantum-classical systems [20, 21] which can also be generalised to situations where the bath follows a non-Hamiltonian dynamics [22, 23].

A simple and efficient algorithm suited for the computer simulation of the quantum-classical Liouville equation is the Sequential Short-Time Propagation (SSTP) algorithm [24]. The SSTP algorithm is based on a first order expansion in time of the Dyson form of the quantum-classical propagator and, when combined with the momentum-jump approximation [25, 26], leads to a representation of non-adiabatic dynamics in terms of piecewise adiabatic trajectories of the bath coordinates, interspersed with stochastic transitions between the energy levels of the subsystem. Despite the similarities to a recently introduced scheme based on a Trotter decomposition of the quantum-classical propagator [28], the basic version of the SSTP algorithm is not as stable at long times and it also displays problems in the region of intermediate and strong coupling to the bath, as illustrated by the results of calculations on the spin-boson model [29–31]. The growth of the statistical error in time can be mitigated by means of filtering schemes. One such a scheme [27] is essentially based on establishing a cutting threshold of the observable when it becomes too large because of the accumulation in time of the sampling weight. Such a scheme will be referred to in the following as the observable-cutting scheme. More recently, another filtering algorithm, which is based on a generalised sampling of non-adiabatic transitions, has been proposed. Such an algorithm has been proven to dramatically reduce the statistical error at long time [30, 31]. This other scheme will be called in this paper as the transition-filtering scheme.

In this work, we use the SSTP algorithm to integrate the quantum-classical Liouville

equation for the spin-boson model and perform a comparison of the performances of the two filtering schemes discussed above. The main result of this paper is that the SSTP algorithm used in conjunction with the combination of the observable-cutting and the transition-filtering schemes performs as well as the Trotter algorithm also in the intermediate and strong coupling regimes. This result is desirable since the SSTP algorithm is easier to implement than its Trotter counterpart, especially when the number of quantum states greater than two must be considered. This promises to be advantageous when studying quantum systems which are more complex than the spin-boson model.

The structure of the paper is as follows. Section II sketches the derivation of the quantum-classical Liouville equation and its representation in the adiabatic basis. In Sec. III the basic version of the SSTP algorithm is illustrated together with the observable-cutting and the transition-filtering schemes. In the same section, the combined filtering scheme is introduced. Section IV discusses the results of the numerical calculations on the dynamics of the spin-boson model using the various filtering schemes. Finally, our conclusions are given in Sec. V.

II. QUANTUM-CLASSICAL LIOUVILLE EQUATION

Let us consider a system that is defined by the following Hamiltonian operator:

$$\hat{H} = \hat{H}_S + \hat{H}_B + \hat{H}_{SB}, \quad (1)$$

where S, B and SB are subscripts denoting the subsystem, bath and the coupling, respectively. The Heisenberg equation of motion for an arbitrary operator \hat{A} can be written in symplectic form as [22]

$$\frac{\partial}{\partial t} \hat{A} = \frac{i}{\hbar} \left[\hat{H} \quad \hat{A} \right] \cdot \mathcal{B}^c \cdot \begin{bmatrix} \hat{H} \\ \hat{A} \end{bmatrix}, \quad (2)$$

where the symplectic matrix [32] \mathcal{B}^c is given by

$$\mathcal{B}^c = \begin{bmatrix} 0 & 1 \\ -1 & 0 \end{bmatrix}. \quad (3)$$

It is assumed that the Hamiltonian of the bath depends on a pair of canonically conjugate operators, $\hat{X} = (\hat{R}, \hat{P})$, and that the coupling Hamiltonian \hat{H}_{SB} depends only on \hat{R} and not

\hat{P} . The partial Wigner transform of the operator \hat{A} over the bath coordinates is

$$\hat{A}_W(X) = \int dz e^{iPz/\hbar} \left\langle R - \frac{z}{2} \left| \hat{A} \right| R + \frac{z}{2} \right\rangle. \quad (4)$$

The partial Wigner transform of the density matrix $\hat{\rho}$ of the system described by the Hamiltonian in Eq. (1) is

$$\hat{\rho}_W(X) = \frac{1}{(2\pi\hbar)^{3N}} \int dz e^{iPz/\hbar} \left\langle R - \frac{z}{2} \left| \hat{\rho} \right| R + \frac{z}{2} \right\rangle, \quad (5)$$

where $X = (R, P)$ are now no longer operators but canonically conjugate classical phase space variables. The partial Wigner transform of the Heisenberg equation of motion can be written in matrix form upon introducing the antisymmetric matrix operator \mathcal{D} given by [22]

$$\mathcal{D} = \begin{bmatrix} 0 & e^{\frac{i\hbar}{2} \overleftarrow{\partial}_k \mathcal{B}_{kj}^c \overrightarrow{\partial}_j} \\ -e^{\frac{i\hbar}{2} \overleftarrow{\partial}_k \mathcal{B}_{kj}^c \overrightarrow{\partial}_j} & 0 \end{bmatrix}. \quad (6)$$

The symbols $\overleftarrow{\partial}_k = \overleftarrow{\partial} / \partial X_k$ and $\overrightarrow{\partial}_k = \overrightarrow{\partial} / \partial X_k$ denote the operators of derivation with respect to the phase-space coordinates acting to the left and right, respectively. The summation over repeated indices must be understood here and in the following. The partial Wigner-transformed Hamiltonian can be written as

$$\hat{H}_W(X) = \hat{H}_S + H_{W,B}(X) + \hat{H}_{W,SB}(R), \quad (7)$$

where we have assumed that the bath dependence of the coupling terms is on positions only:

$$\hat{H}_{W,SB} = V_B(R) \otimes \hat{H}'_S, \quad (8)$$

where H'_S acts only in the Hilbert space of the subsystem. The above representation is equivalent to the Heisenberg representation, but in general calculations are difficult to perform. However, in many instances a quantum-classical approximation can be taken by means of a linear expansion of the exponential terms in the \mathcal{D} matrix, giving

$$\mathcal{D}_{lin} = \begin{bmatrix} 0 & 1 + \frac{i\hbar}{2} \overleftarrow{\partial}_k \mathcal{B}_{kj}^c \overrightarrow{\partial}_j \\ -1 - \frac{i\hbar}{2} \overleftarrow{\partial}_k \mathcal{B}_{kj}^c \overrightarrow{\partial}_j & 0 \end{bmatrix}. \quad (9)$$

This allows one to write the quantum-classical Liouville equation as

$$\begin{aligned} \frac{\partial}{\partial t} \hat{A}(X, t) &= \frac{i}{\hbar} \left[\hat{H}_W(X) \hat{A}_W(X, t) \right] \cdot \mathcal{D}_{lin} \\ &\cdot \begin{bmatrix} \hat{H}_W(X) \\ \hat{A}_W(X, t) \end{bmatrix}. \end{aligned} \quad (10)$$

When $V_B(R)$ is linear in R and $H_{W,B}$ is quadratic in the bath coordinates the linear expansion is exact ($\mathcal{D}_{lin} = \mathcal{D}$) and quantum-classical dynamics is equivalent to full quantum dynamics.

In order to perform calculations, Eq. (10) must be represented in a basis. The adiabatic basis leads naturally to a splitting of non-adiabatic and adiabatic terms, which is ideal for surface-hopping algorithms. The adiabatic basis is defined as the solution to the eigenvalue equation

$$\hat{h}(R)|\alpha; R\rangle = E_\alpha(R)|\alpha; R\rangle. \quad (11)$$

In this basis the quantum-classical evolution takes the form

$$A_W^{\alpha\alpha'}(X, t) = \sum_{\beta\beta'} (e^{it\mathcal{L}})_{\alpha\alpha',\beta\beta'} A_W^{\beta\beta'}(X), \quad (12)$$

where the quantum-classical Liouville operator [14] is given by

$$\begin{aligned} i\mathcal{L}_{\alpha\alpha',\beta\beta'} &= (i\omega_{\alpha\alpha'} + iL_{\alpha\alpha'}) \delta_{\alpha\beta} \delta_{\alpha'\beta'} + J_{\alpha\alpha',\beta\beta'}^{\text{MJ}} \\ &= i\mathcal{L}_{\alpha\alpha'}^0 \delta_{\alpha\beta} \delta_{\alpha'\beta'} + J_{\alpha\alpha',\beta\beta'}^{\text{MJ}}, \end{aligned} \quad (13)$$

where the MJ superscript denotes that we have used the momentum-jump approximation [25, 26]. The Bohr frequency is defined as

$$\omega_{\alpha\alpha'}(R) = \frac{E_\alpha(R) - E_{\alpha'}(R)}{\hbar}, \quad (14)$$

and the classical-like Liouville operator for the bath degrees of freedom is given by

$$iL_{\alpha\alpha'} = \frac{P}{M} \cdot \frac{\partial}{\partial R} + \frac{1}{2}(F_W^\alpha + F_W^{\alpha'}) \cdot \frac{\partial}{\partial P}, \quad (15)$$

where F_W^α and $F_W^{\alpha'}$ are the Hellman-Feynman forces for adiabatic energy surface E_α and $E_{\alpha'}$ respectively.

The operator $J_{\alpha\alpha',\beta\beta'}^{\text{MJ}}$ is known as the transition operator in the momentum-jump approximation [25, 26], and is responsible for the non-adiabatic transitions in the quantum subsystem and the accompanying changes in the bath momentum. It is given by

$$J_{\alpha\alpha',\beta\beta'}^{\text{MJ}} = \mathcal{T}_{\alpha \rightarrow \beta}^{\text{MJ}} \delta_{\alpha'\beta} + \mathcal{T}_{\alpha' \rightarrow \beta'}^{\text{MJ}*} \delta_{\alpha\beta}, \quad (16)$$

where

$$\mathcal{T}_{\alpha \rightarrow \beta}^{\text{MJ}} = \frac{P}{M} \cdot d_{\alpha\beta}(R) \exp \left[\frac{1}{2} \frac{\Delta E_{\alpha\beta}(R) d_{\alpha\beta}(R)}{\frac{P}{M} \cdot d_{\alpha\beta}(R)} \cdot \frac{\partial}{\partial P} \right]. \quad (17)$$

In the momentum-jump approximation the back-reaction on the bath (i.e., the change to bath momenta) accompanying a non-adiabatic transition can be calculated analytically. If we consider an $\alpha \rightarrow \beta$ transition, the momentum-shift approximated J operator, J^{MJ} , produces a shift in the bath momenta P . This shift is defined as

$$P \rightarrow P' = P + \Delta_{\alpha\beta}^{\text{MJ}} P, \quad (18)$$

where

$$\begin{aligned} \Delta_{\alpha\beta}^{\text{MJ}} P &= -(P \cdot \hat{d}_{\alpha\beta}) \hat{d}_{\alpha\beta} \\ &+ \hat{d}_{\alpha\beta} \text{sign}(P \cdot \hat{d}_{\alpha\beta}) \sqrt{(P \cdot \hat{d}_{\alpha\beta})^2 + M \Delta E_{\alpha\beta}}. \end{aligned} \quad (19)$$

The symbol $\hat{d}_{\alpha\beta}$ is the unit vector associated with the coupling vector in the multidimensional space of all the particle coordinates. Note that in the above, we have assumed that all the masses are the same, however, it is a simple matter to extend this to a system where the masses are different. If we expand the square root on the right-hand side of equation (19), we obtain the approximated form for the momentum shift rule

$$\tilde{\Delta}_{\alpha\beta}^{\text{MJ}} P = \frac{1}{2} \frac{\Delta E_{\alpha\beta}(R)}{\frac{P}{M} \cdot \hat{d}_{\alpha\beta}} \hat{d}_{\alpha\beta}. \quad (20)$$

Note that while the exact momentum shift in equation (19) exactly conserves the energy, the approximated form in equation (20) does not. In our calculations, only the exact form of the momentum shift was used.

III. FILTERING SCHEMES FOR THE SSTP ALGORITHM

The SSTP algorithm is derived upon considering the evolution along a quantum-classical trajectory given by the solution of Eq. (12) as a series of sequential small time steps τ . Hence, the short-time expression of the quantum-classical propagator $[\exp(i\tau \mathcal{L}^{\text{MJ}})]_{\alpha\alpha',\beta\beta'}$ is approximated to linear order in time as

$$\begin{aligned} &e^{i\tau \mathcal{L}_{\alpha\alpha'}^0} (\delta_{\alpha\beta} \delta_{\alpha'\beta'} + \tau J_{\alpha\alpha',\beta\beta'}^{\text{MJ}}) \\ &= \mathcal{W}_{\alpha\alpha'}(\tau) e^{iL_{\alpha\alpha'}\tau} (\delta_{\alpha\beta} \delta_{\alpha'\beta'} + \tau J_{\alpha\alpha',\beta\beta'}^{\text{MJ}}). \end{aligned} \quad (21)$$

In the limit $\tau \rightarrow 0$, the concatenation of the short time steps exactly reproduces the Dyson integral expansion of the operator $\exp(i\tau\mathcal{L})_{\alpha\alpha',\beta\beta'}$ for finite times [24]. The computational evaluation of each single step τ can be evaluated upon considering the short time propagator in Eq. (21) as a stochastic operator. The action of the transition operator $J_{\alpha\alpha',\beta\beta'}^{\text{MJ}}$ is then sampled using a suitable transition probability. This transition probability is not uniquely fixed but has to be chosen following the criteria of physical reasonability and computational efficiency.

The transition probability is defined as the probability of a non-adiabatic transition occurring in a time interval τ . A basic choice for this probability is given by

$$\mathcal{P}_{\alpha\beta}^0(X, \tau) = \frac{\tau \left| \frac{P}{M} \cdot d_{\alpha\beta}(R) \right|}{1 + \tau \left| \frac{P}{M} \cdot d_{\alpha\beta}(R) \right|}. \quad (22)$$

This transition probability then defines the probability of no transition occurring in the same time interval as

$$\begin{aligned} \mathcal{Q}_{\alpha\beta}^0(X, \tau) &= 1 - \mathcal{P}_{\alpha\beta}^0 \\ &= \frac{1}{1 + \tau \left| \frac{P}{M} \cdot d_{\alpha\beta}(R) \right|}. \end{aligned} \quad (23)$$

when at time step i in the calculation the transition probability is sampled, and a transition occurs, the observable is multiplied by a factor of $(P/M) \cdot d_{\alpha\beta} (\mathcal{P}_{\alpha\beta}^0)^{-1}$. If no transition occurs, then the observable is multiplied by a factor of $(\mathcal{Q}_{\alpha\beta}^0)^{-1}$. The $(P/M) \cdot d_{\alpha\beta}$ term introduced when a transition occurs originates from the action of the $J_{\alpha\alpha',\beta\beta'}^{\text{MJ}}$ operator. The concatenation of these factors result in a weight in the observable which causes an error in the result at longer times. We thus need to sample non-adiabatic transitions in such a way that minimises this statistical error.

The first method for reducing statistical error tackles the problem directly. It is a simple but effective approach. As mentioned above, the magnitude of the weight, which is used to calculate the observable, grows with time and causes the value of the observable to grow, leading to large statistical error. Knowing this, we can introduce a threshold value c_t which sets an upper bound to the magnitude of the weight. If at a stage j in the calculation of a trajectory we have that the magnitude of the weight W becomes larger than c_t , it is instead set to the value of c_t . Mathematically, we can write this as:

$$W = \begin{cases} W & \text{if } |W| < c_t \\ \text{sign}(W)c_t & \text{if } |W| > c_t \end{cases} \quad (24)$$

Note that this cutting only affects the magnitude of the weight, the sign remains the same. This cutting ensures that the weight can never grow to values where a single trajectory is having an overly large effect on the value of the observable. Consequently, we do not see the large statistical error in the result at longer times. While effective, however, this scheme does not have any physical basis, unlike the transition filtering scheme.

Another approach to the reduction of the statistical error has been recently proposed in Refs. [30, 31]. Essentially, It is based on filtering out those non-adiabatic transitions which would lead to too big a change in the momenta. In order to illustrate such an approach, it is useful to recall the form of the energy variation because of a non-adiabatic transition calculated using an approximate form of the momentum-shift rule:

$$\mathcal{E}_{\alpha\beta} = \frac{P'^2}{2M} + E_{\alpha}(R) - \left(\frac{P^2}{2M} + E_{\beta}(R) \right), \quad (25)$$

where $P' = P + \tilde{\Delta}_{\alpha\beta}^{\text{MJ}}P$. Upon introducing the parameter $c_{\mathcal{E}}$ and the weight $\omega(c_{\mathcal{E}}, \mathcal{E}_{\alpha\beta})$, one can define a generalised transition probability

$$\mathcal{P}_{\alpha\beta}^{EC}(X, \tau) = \frac{\tau \left| \frac{P}{M} \cdot d_{\alpha\beta}(R) \right| \omega(c_{\mathcal{E}}, \mathcal{E}_{\alpha\beta})}{1 + \tau \left| \frac{P}{M} \cdot d_{\alpha\beta}(R) \right| \omega(c_{\mathcal{E}}, \mathcal{E}_{\alpha\beta})}. \quad (26)$$

This in turn defines the probability of no transition occurring as

$$\begin{aligned} \mathcal{Q}_{\alpha\beta}(X, \tau) &= 1 - \mathcal{P}_{\alpha\beta}^{EC} \\ &= \frac{1}{1 + \tau \left| \frac{P}{M} \cdot d_{\alpha\beta}(R) \right| \omega(c_{\mathcal{E}}, \mathcal{E}_{\alpha\beta})}. \end{aligned} \quad (27)$$

The weight $\omega(c_{\mathcal{E}}, \mathcal{E}_{\alpha\beta})$ is defined as

$$\omega(c_{\mathcal{E}}, \mathcal{E}_{\alpha\beta}) = \begin{cases} 1 & \text{if } \mathcal{E}_{ab} \leq c_{\mathcal{E}}, \\ 0 & \text{otherwise.} \end{cases} \quad (28)$$

The transition probabilities in Eqs. (26) and (27) allow one to control the amplitude of energy fluctuations that would be caused by an approximate momentum shift through the use of the numerical parameter $c_{\mathcal{E}}$. Whenever a non-adiabatic transition would cause a virtual energy fluctuation that is larger than $c_{\mathcal{E}}$, the transition probability becomes zero, and no transition can occur. This generalisation of the basic sampling scheme allows non-adiabatic transitions to occur only in regions where the approximate momentum shift rule causes small virtual variation of the energy of the system: this happens when the change

in the momentum is not too big. Such a scheme has been proven numerically to be very efficient in reducing statistical error at long times [30, 31].

Since each of the above filtering techniques approach the statistical error problem from different angles, it is interesting to combine them within a single simulation algorithms. According to such an idea, in each simulation, the non-adiabatic transitions are filtered according to the transition-filtering scheme, using the parameter $c_{\mathcal{E}}$, in addition to the observable being cut when it grows too large, according to the parameter c_t .

IV. NUMERICAL CALCULATIONS

Our numerical study was performed on the spin-boson model [33], which can be considered as a paradigmatic example for quantum dynamics [29] for which the adiabatic states are known exactly. Such a system comprises a single spin coupled to a bath of harmonic oscillators. Using adimensional coordinates [24, 28, 29], the spin-boson Hamiltonian is given by defining the various terms in Eq. (7) as

$$\hat{H}_S = -\Omega\hat{\sigma}_x, \quad (29)$$

$$H_{W,B} = \sum_{i=1}^N \left(\frac{P_i^2}{2M_i} + \frac{1}{2}M_i\omega_i^2 R_i^2 \right), \quad (30)$$

$$\hat{H}_{W,SB} = -\sum_{i=1}^N c_i R_i \hat{\sigma}_z, \quad (31)$$

where $\hat{\sigma}_x$ and $\hat{\sigma}_z$ are the Pauli spin matrices and c_i are the coupling coefficients. These coefficients are determined by requiring that the system spectral density is Ohmic [34].

In simulations, we have set the spin in an excited state at $t = 0$, and the quantum harmonic modes are at thermal equilibrium, with no coupling before $t = 0$. After $t = 0$, the coupling is switched on, and we calculate the observable $\langle \hat{\sigma}_z(t) \rangle$, or population difference of the system. We have considered $n = 2$ non-adiabatic transitions per trajectory, as this was sufficient for the results to converge. Each simulation used a total of $N_{\text{mcs}} = 10^5$ sampled phase space points for the initial conditions. The integration time step was $dt = 0.1$ in dimensionless units.

Figures 1 and 2 give the results for weak coupling, with system parameters $\beta = 0.3$, $\xi = 0.007$, and $\Omega = 1/3$. From Figs. 1 and 2, we see that both filtering techniques give results that agree well with the influence functional path integral calculations [34], however,

the two results deviate from each other at longer times. For both cases we can observe the growth of the statistical error at longer times, although it is relatively minimal for weak coupling. Figure 3 displays the weak coupling result for the combined filtering scheme. In this case we again see the excellent agreement with the influence functional results, but the error bars are smaller than the points for the entire simulation time. Moreover, the calculation remains stable for longer times [30, 31] than those obtained in previously published results.

Figures 4 and 5 show the results for mid-range coupling. The system parameters used were $\beta = 12.5$, $\xi = 0.09$ and $\Omega = 0.4$. Figures 4 and 5 give the comparison of the two filtering schemes. The results for both filtering schemes agree very well with the exact quantum result from Ref. [34] up until approximately $t = 20$, but after this time the results deviate somewhat. In the case of the transition-sampling filter, we do not observe the damping that occurs in the exact result - the oscillations remain large. For the observable-cutting scheme, however, we see the opposite. The observable-cutting filter damps the result too much at longer times, causing it to become zero. In Fig. 6, we have the result for the combined filtering scheme. We see a dramatic improvement over both the individual filtering scheme, since the combined filter does not exhibit either of the problems observed above. The combined filtering result agrees far better with the exact quantum result at longer times, with the error bars smaller than the points for the entire simulation time.

In Figs. 7 and 8 the results for strong coupling are presented. For these results we adopted the system parameters $\beta = 0.25$, $\xi = 2.0$ and $\Omega = 1.2$. From Figs. 7 and 8 we can see that the two filtering schemes are incapable of reproducing the exact quantum results of Ref. [35] at even short times. Although both schemes are successful at reducing the statistical error, we do see that the error bars become larger than the points at approximately $t = 2$. In Fig. 9 we show the result obtained with the combined filtering scheme for strong coupling. Again, the improvement is remarkable. In the main figure, an excellent agreement with the exact quantum result is illustrated, while the inset shows that the result can be extended to long times with statistical error remaining smaller than the points.

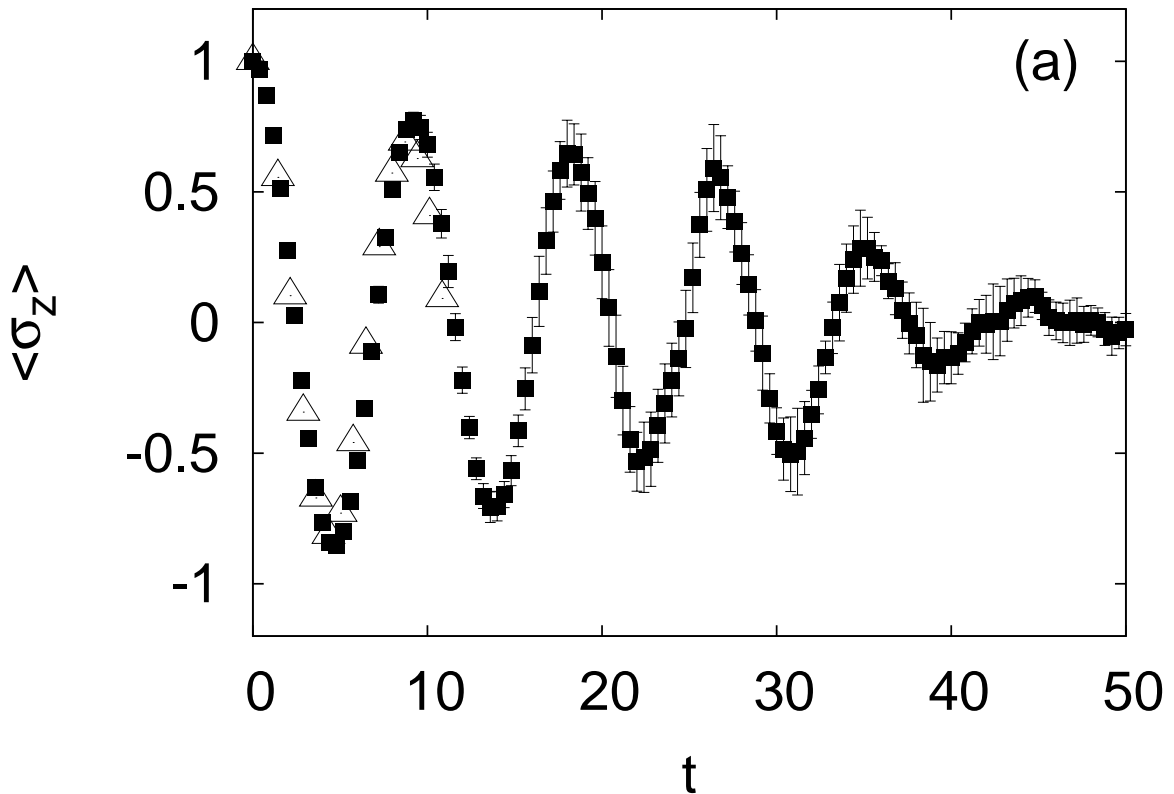


FIG. 1: Comparison of the SSTP results with the observable-cutting (■) and the transition-filtering algorithm (◆, panel b) to exact quantum results (△). System parameters were $\beta = 0.3$, $\xi = 0.007$, $\Omega = 1/3$, corresponding to weak coupling. The value of the threshold parameter for the observable-cutting was $c_t = 100.0$. Two non-adiabatic transitions were included in the calculations.

V. CONCLUSIONS

We have studied three different methods for reducing the statistical error when simulating the quantum-classical Liouville approach to non-adiabatic dynamics by means of the Sequential Short-Time Step algorithm [24]. The first two methods are the observable-cutting scheme (which uses the reset to threshold value for the statistical weights entering the definition of the observable) and the transition-filtering approach (which prunes the ensemble of allowed non-adiabatic transitions on the basis of a generalised sampling probability). We have used the spin-boson model as a paradigmatic example of quantum dynamics in a dissipative environment [33] and performed numerical calculations on the evolution in time of the

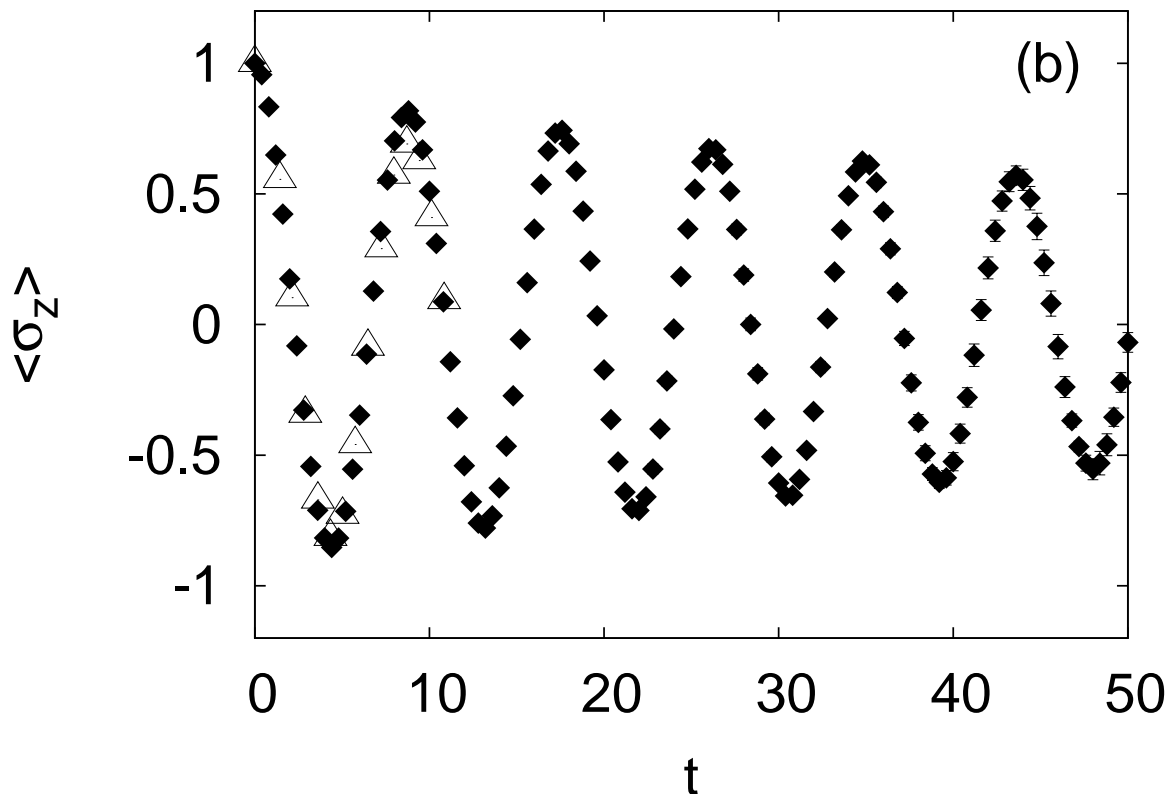


FIG. 2: Comparison of the transition-filtering results (\blacklozenge) to exact quantum results (\triangle). System parameters were $\beta = 0.3$, $\xi = 0.007$, $\Omega = 1/3$, corresponding to weak coupling. The value of the threshold parameter for the observable-cutting was $c_t = 100.0$, and the value of the control parameter for the energy conserving filtering was $c_\varepsilon = 0.005$. Two non-adiabatic transitions were included in the calculations.

state population difference of this model. The use of either scheme gives rise to results that have smaller statistical error than those obtained when using the basic sampling, and both filtering techniques are capable of producing results in good agreement with the numerically exact quantum results for short times, but only for the intermediate and weak coupling regimes. Although both schemes are an improvement over the basic sampling method in the SSTP algorithm, they are still unable to reproduce the numerically exact results for strong coupling, and fail at longer times for intermediate coupling as well. Moreover, both schemes, when used in separation from the other, are not able to curb the increase of the statistical error at longer times.

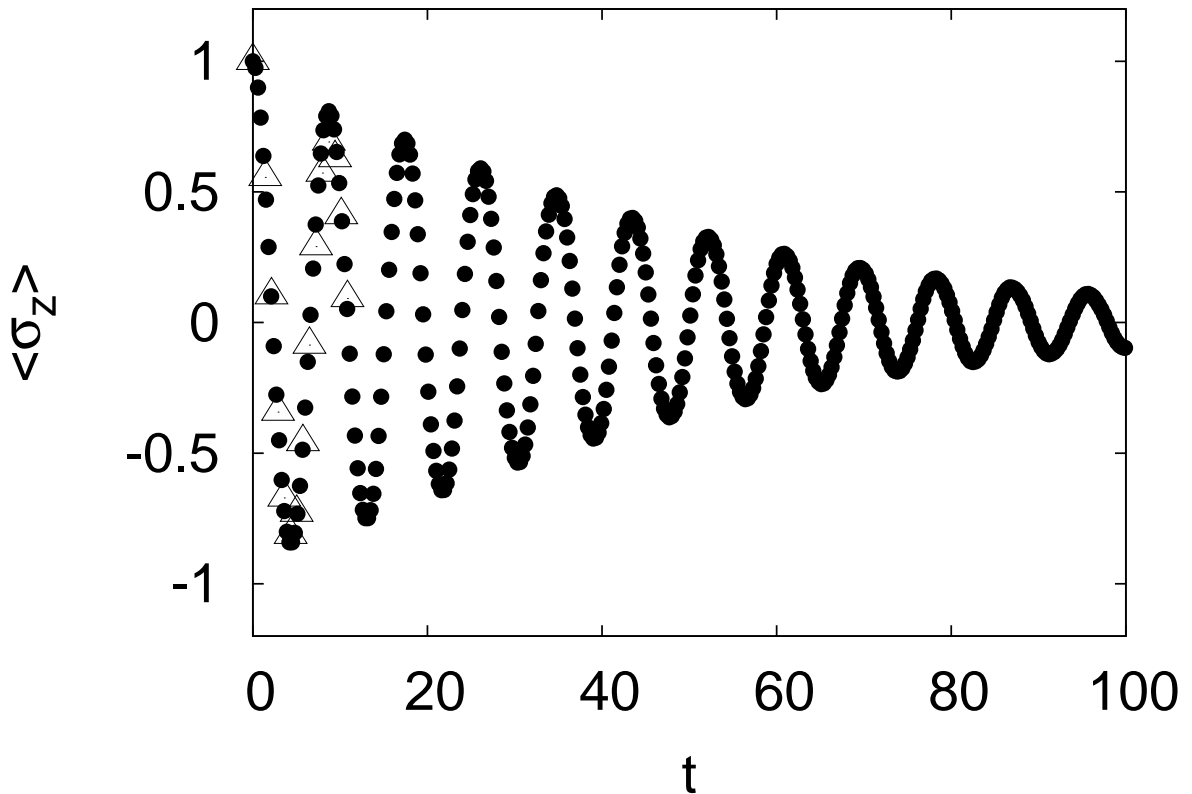


FIG. 3: Comparison of the SSTP with the combined filtering algorithm (\bullet) to exact quantum results (\triangle). System parameters were $\beta = 0.3$, $\xi = 0.007$, $\Omega = 1/3$. The value of the threshold parameter was $c_t = 1.5$, and the value of the energy conserving filtering control parameter was $c_\varepsilon = 0.005$. Two non-adiabatic transitions were included in the calculations.

Nevertheless, we have shown that the combination of these two filtering methods in a single scheme solve both of the problems encountered by the individual filtering schemes. This is the main result of this paper. Upon using the combined filtering scheme, we have produced results that not only have negligible statistical error for longer simulation time than that accessible in previously published calculations, but compare far more favorably with the numerically exact results. The combined method is able to nearly perfectly reproduce the strong coupling results, whereas the individual schemes could not do this even at very short times. Our results are also as good as those obtained with the Trotter-based algorithm for the simulation of the quantum-classical Liouville equation [28]. However, since the SSTP algorithm is easier to implement for systems which have a number of quantum states greater

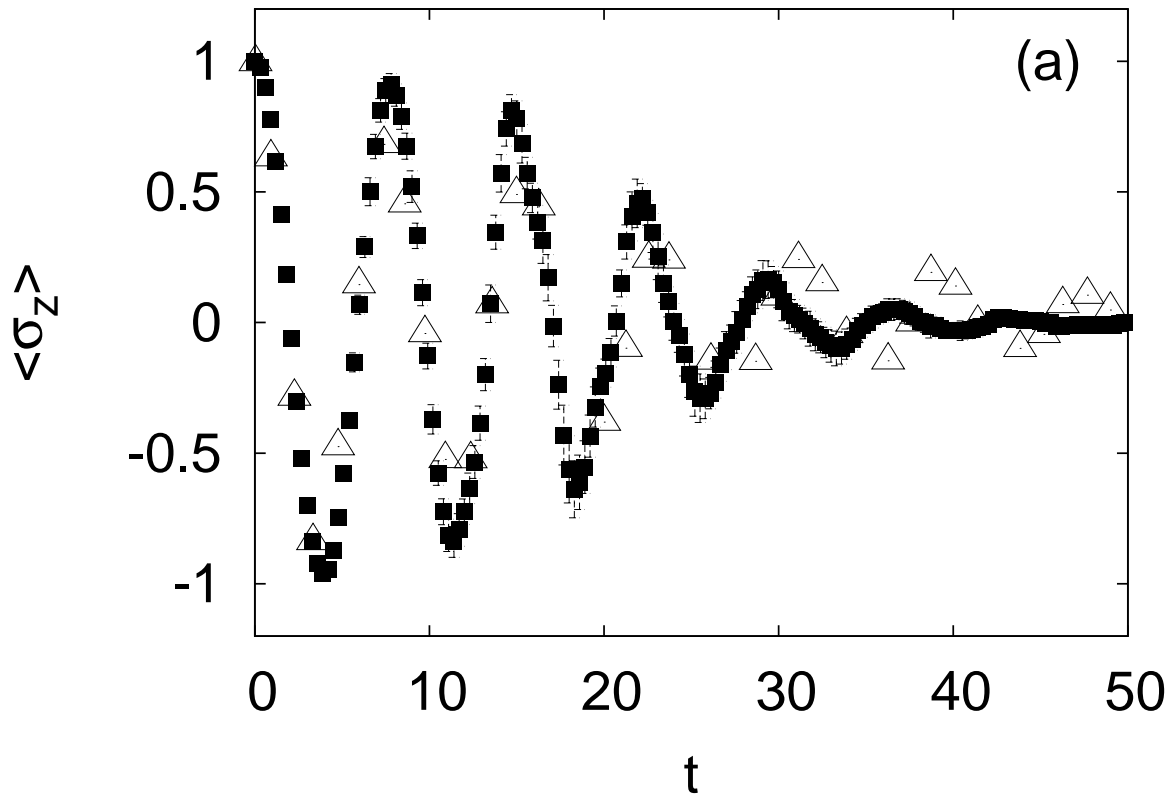


FIG. 4: Comparison of the SPTP with the observable-cutting (■) to exact quantum results (△). System parameters were $\beta = 12.5$, $\xi = 0.09$, $\Omega = 0.4$, corresponding to mid-range coupling. The value of the threshold parameter for the direct filtering was $c_t = 50.0$. Two non-adiabatic transitions were included in the calculations.

than two, our proposal of the combined filtering scheme promises to be advantageous for more complex numerical studies of non-adiabatic dynamics.

Acknowledgements

This work is based upon research supported by the South African Research Chair Initiative of the Department of Science and Technology and the National Research Foundation.

[1] I. V. Aleksandrov, Z. Naturforsch. A **36A**, 902 (1981).

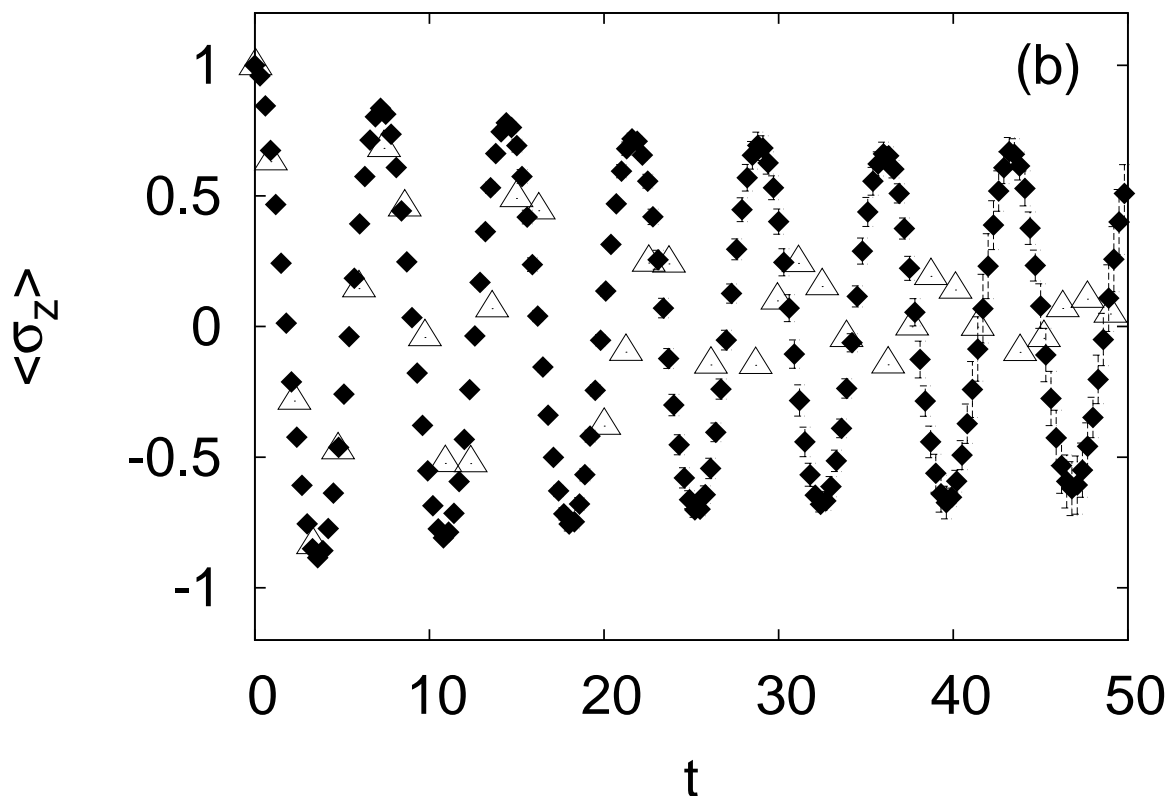


FIG. 5: Comparison of the transition-filtering algorithm (\blacklozenge) to exact quantum results (\triangle). System parameters were $\beta = 12.5$, $\xi = 0.09$, $\Omega = 0.4$, corresponding to mid-range coupling. The value of the control parameter was $c_{\mathcal{E}} = 0.025$. Two non-adiabatic transitions were included in the calculations.

- [2] V. I. Gerasimenko, *Theor. Math. Phys.* **50**, 77 (1982).
- [3] W. Boucher and J. Traschen, *Phys. Rev. D* **37** 3522 (1988).
- [4] W. Y. Zhang and R. Balescu, *J. Plasma Phys.* **40**, 199 (1988).
- [5] R. Balescu and W. Y. Zhang, *J. Plasma Physics* **40**, 215 (1988).
- [6] J. C. Tull and R. K. Preston, *J. Chem. Phys.* **55** 562 (1971).
- [7] W. H. Miller and F. F. George, *J. Chem. Phys.* **56** 5637 (1972).
- [8] P. Pechukas, *Phys. Rev.* **181** 166 (1969).
- [9] P. Pechukas, *Phys. Rev.* **174** 166 (1969).
- [10] E. J. Heller, B. Segev, and A. V. Sergeev, *J. Phys. Chem. B* **106** 8471 (2002).
- [11] N. Shenvi, *J. Chem. Phys.* **130** 124177 (2009).

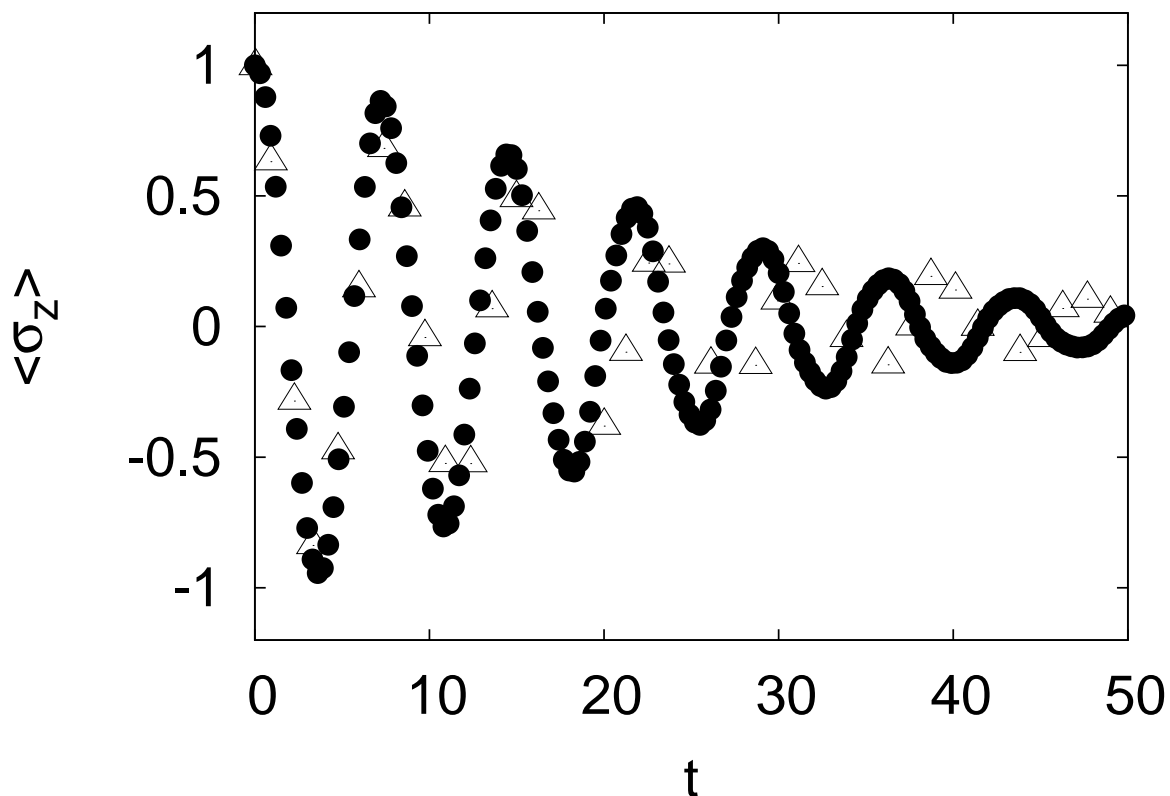


FIG. 6: Comparison of the SSTP with the combined filtering algorithm (●) to exact quantum results (△). System parameters were $\beta = 12.5$, $\xi = 0.09$, $\Omega = 0.4$. The value of the threshold parameter was $c_t = 3.5$, and the value of the control parameter was $c_\xi = 0.05$. Two non-adiabatic transitions were included in the calculations.

- [12] Classical and Quantum Dynamics in the Condensed Phase Simulations, B. J. Berne, G. Ciccotti, and D. Coker eds. (World Scientific, Singapore, 1998).
- [13] C. C. Martens and J.-Y. Fang, *J. Chem. Phys.* **106**, (1996) 4918.
- [14] R. Kapral and G. Ciccotti, *J. Chem. Phys.* **110**, (1999) 8919.
- [15] I. Horenko, C. Salzmann, B. Schmidt, and C. Schutte, *J. Chem. Phys.* **117**, (2002) 11075.
- [16] Q. Shi and E. Geva, *J. Chem. Phys.* **121**, (2004) 3393.
- [17] A. Sergi, I. Sinayskiy, and F. Petruccione, *Physical Review A* **80**, 012108 (2009).
- [18] N. Rejik, C.-Yu Hsieh, H. Freedman, and G. Hanna, *J. Chem. Phys.* **138**, 144106 (2013).
- [19] Qiang Shi and Eitan Geva, *J. Chem. Phys.* **131**, 034511 (2009).
- [20] S. Nielsen, R. Kapral, and G. Ciccotti, *J. Chem. Phys.* **115**, 5805 (2001).

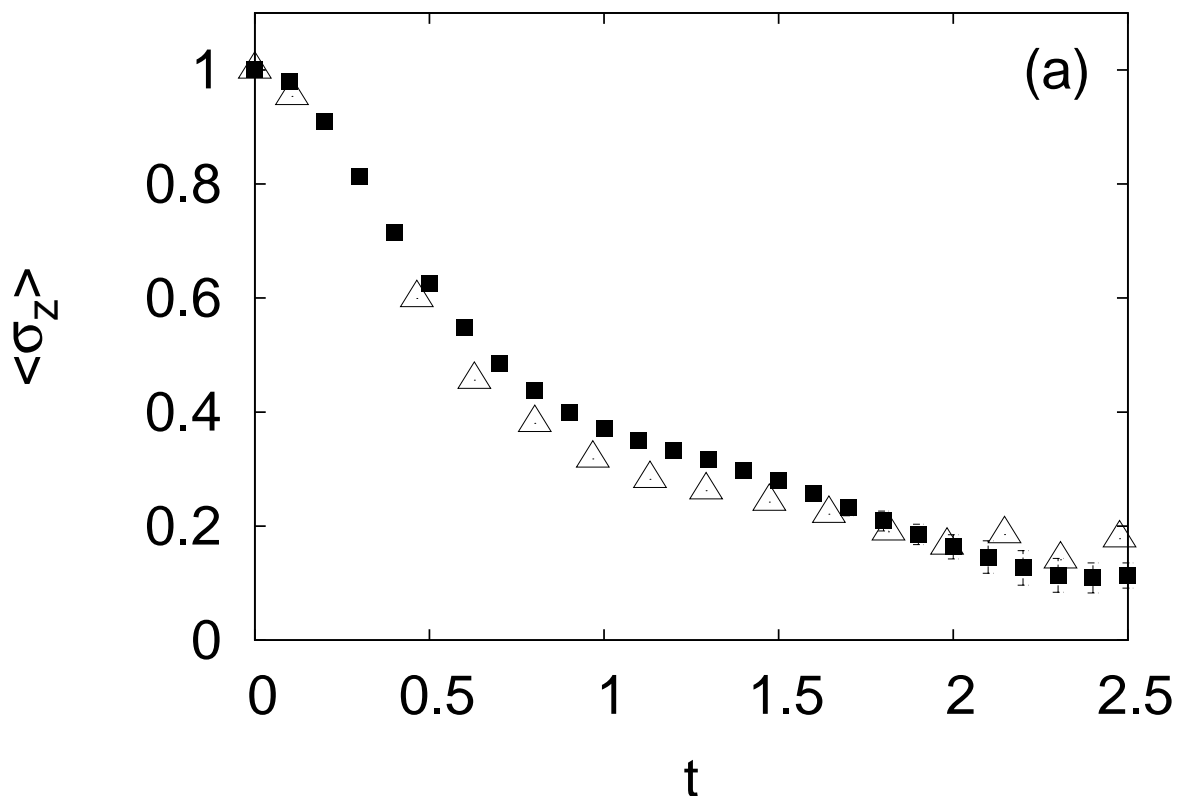


FIG. 7: Comparison of the SSTP with the observable-cutting (■) to exact quantum results (Δ). System parameters were $\beta = 0.25$, $\xi = 2.0$, $\Omega = 1.2$, corresponding to high coupling. The value of the bound parameter for the direct filtering was $c_t = 50.0$. Two non-adiabatic transitions were included in the calculations.

- [21] A. Sergi, J. Chem. Phys. **124**, 024110 (2006).
- [22] A. Sergi, Phys. Rev. E **72**, 066125 (2005).
- [23] A. Sergi, J. Phys. A: Math. Theor. **40**, F347 (2007).
- [24] D. MacKernan, R. Kapral, and G. Ciccotti, Sequential short-time propagation of quantum-classical dynamics, J. Phys: Condens. Matter **14** 9069 (2002).
- [25] A. Sergi, D. Mac Kernan, G. Ciccotti, and R. Kapral, Theor. Chem. Acc. **110** 49 (2003).
- [26] R. Kapral and G. Ciccotti, in: Bridging time scales: Molecular simulations for the next decade, p 445. P. Nielaba, M. Mareschal, and G. Ciccotti (eds). SIMU Conference 2001. (Springer, Berlin, 2003).
- [27] G. Hanna and R. Kapral, J. Chem. Phys. **122** 244505 (2005).

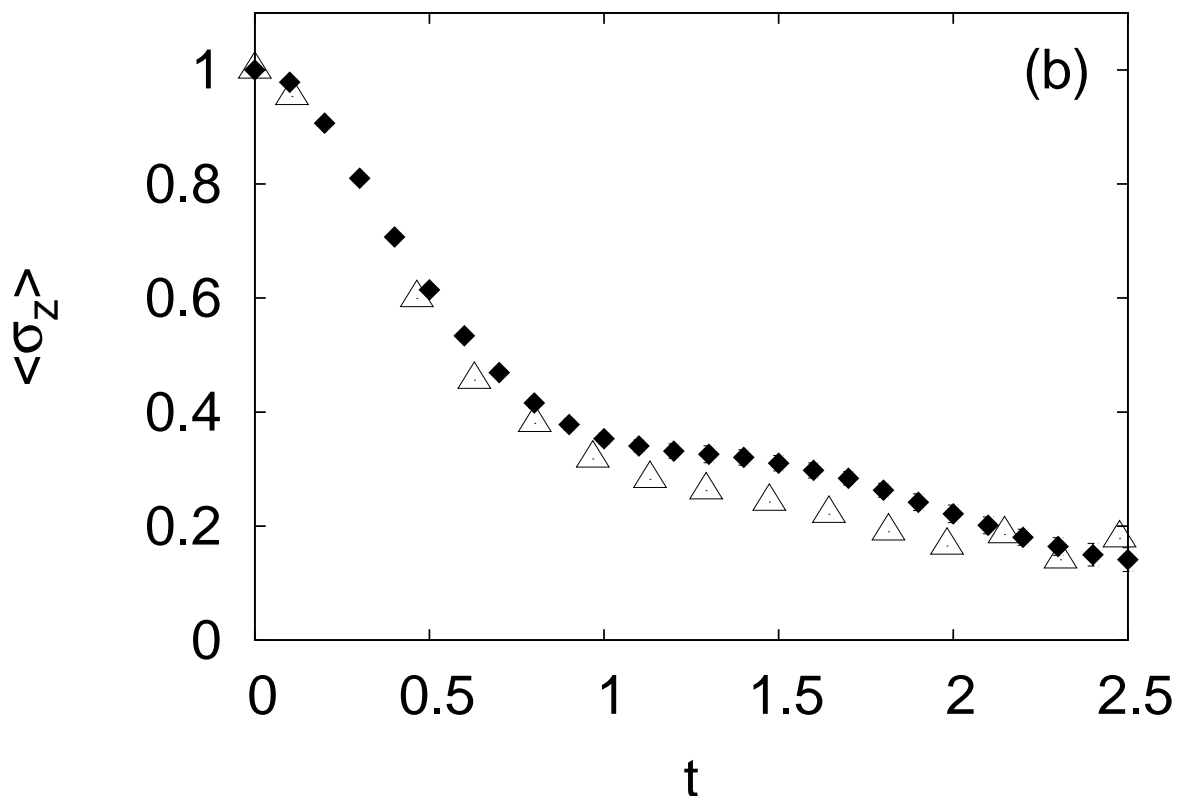


FIG. 8: Comparison of the transition-filtering algorithm (\blacklozenge , panel b) to exact quantum results (\triangle). System parameters were $\beta = 0.25$, $\xi = 2.0$, $\Omega = 1.2$, corresponding to high coupling. The value of the control parameter was $c_\varepsilon = 0.5$. Two non-adiabatic transitions were included in the calculations.

- [28] D. Mac Kernan, G. Ciccotti, and R. Kapral, Trotter-Based Simulation of Quantum-Classical Dynamics, *J. Phys. Chem. B* **112** 424 (2008).
- [29] A. Sergi, D. MacKernan, G. Ciccotti, and R. Kapral, *Theor. Chem. Acc* **110** 49 (2003).
- [30] A. Sergi and F. Petruccione, *Phys. Rev. E* **81** 032101 (2010).
- [31] D. A. Uken, A. Sergi, and F. Petruccione, *Phys. Scr.* **T143** 014024 (2011).
- [32] H. Goldstein, *Classical Mechanics* (Addison-Wesley, Reading, 1980).
- [33] A. J. Leggett, S. Chakravarty, A. T. Dorsey, M. P. A. Fischer, A. Garg, and M. Zwerger, *Rev. Mod. Phys.* **59** 1 (1987).
- [34] D. E. Makarov and N. Makri, *Chem. Phys. Lett.* **221** 482 (1994).
- [35] A. A. Golosov and D. R. Reichman, *J. Chem. Phys.* **114** 1065 (2001).

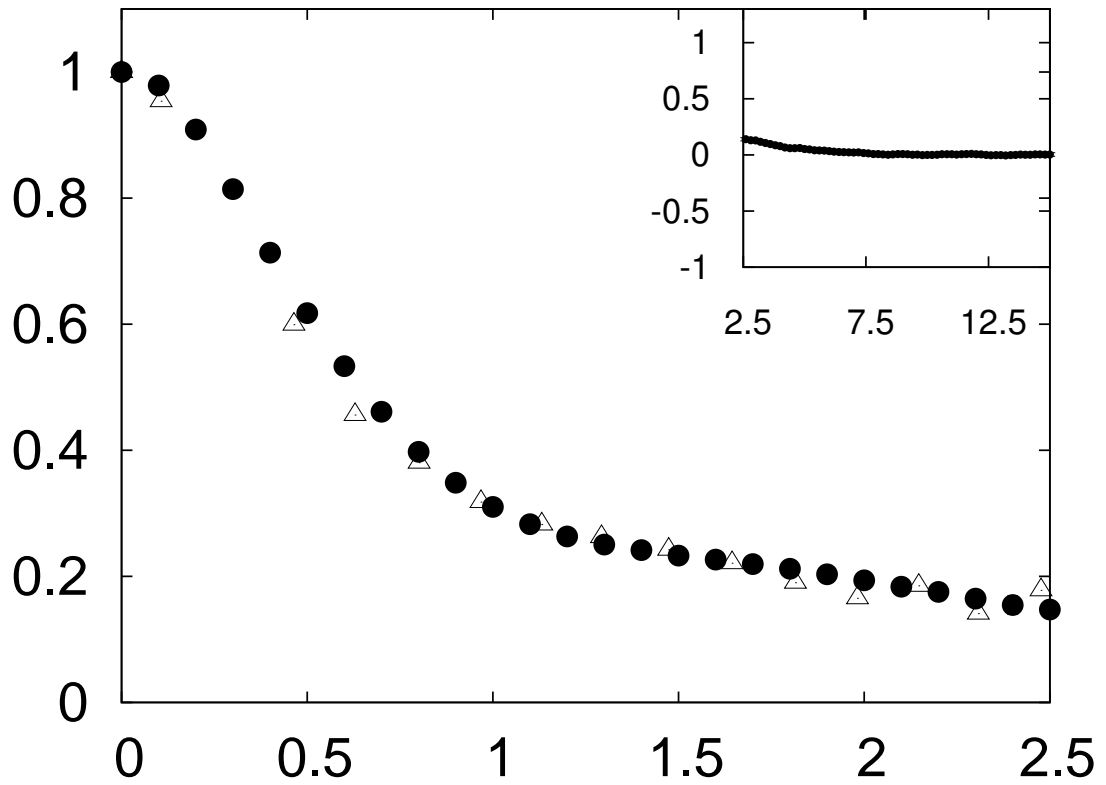


FIG. 9: Comparison of the SSTP with the combined filtering algorithm (●) to exact quantum results (△). System parameters were $\beta = 0.25$, $\xi = 2.0$, $\Omega = 1.2$. The value of the threshold parameter was $c_t = 5.0$, and the value of the control parameter was $c_\xi = 1.0$. Two non-adiabatic transitions were included in the calculations.